Weak magnetism of Aurivillius-type multiferroic thin films probed by polarized neutron reflectivity

Xiaofang Zhai,[1] Alexander J. Grutter,[2,*] Yu Yun,[1,3] Zhangzhang Cui,[1] and Yalin Lu[1,4,†]

[1]*Hefei National Laboratory for Physical Sciences at Microscale, University of Science and Technology of China, Hefei, Anhui 230026, China*

[2]*NIST Center for Neutron Research, National Institute of Standards and Technology, Gaithersburg, Maryland 20899, USA*

[3]*International Center for Quantum Materials, School of Physics, Peking University, Beijing 100871, China*

[4]*National Synchrotron Radiation Laboratory, University of Science and Technology of China, Hefei, Anhui 230026, China*

(Received 12 January 2018; published 27 April 2018)

Unambiguous magnetic characterization of room-temperature multiferroic materials remains challenging due in part to the difficulty of distinguishing their very weak ferromagnetism from magnetic impurity phases and other contaminants. In this study, we used polarized neutron reflectivity to probe the magnetization of $Bi_6FeCoTi_3O_{18}$ and $LaBi_5FeCoTi_3O_{18}$ in their epitaxial thin films while eliminating a variety of impurity contributions. Our results show that $LaBi_5FeCoTi_3O_{18}$ exhibits a magnetization of about $0.016 \pm 0.027\,\mu_B$/Fe-Co pair at room temperature, while the $Bi_6FeCoTi_3O_{18}$ thin film only exhibits a weak magnetic moment below room temperature, with a saturation magnetization of $0.049 \pm 0.015\,\mu_B$/Fe-Co pair at 50 K. This polarized-neutron-reflectivity study places an upper magnetization limit on the matrix material of the magnetically doped Aurivillius oxides and helps to clarify the true mechanism behind the room-temperature magnetic performance.

DOI: 10.1103/PhysRevMaterials.2.044405

Room-temperature (RT) multiferroic materials are promising candidate materials for next-generation device applications, but these systems are rarely identified due to inherent competition between the interactions which stabilize magnetism and ferroelectricity (FE) [1–3]. Only a handful of RT multiferroic systems have been identified thus far, the majority of which exhibit antiferromagnetism (AFM) [4–6] or very weak ferromagnetism (FM) [7–19]. Thus, the detection and unambiguous identification of the weak magnetic moments remains an ongoing challenge. Doped Aurivillius-type systems based on the parent compound $Bi_{n+1}Fe_{n-3}Ti_3O_{3n+3}$ (BFTO) have recently emerged as candidate multiferroic material systems [13,20–38]. Undoped BFTO exhibits a FE polarization aligned parallel to the layer, but is not FM [39–41]. Upon doping with other magnetic elements, such as Co [13,20–33], Mn [32–35], Ni [36,37], Cr [38], etc., Aurivillius materials have been reported to exhibit FM and FE simultaneously at or above the RT. Moreover, RT or high-temperature magnetoelectric coupling was detected in the Co- [26,30] and Mn-doped phases [32,34]. However, the nature of the multiferroicity in this material system is the subject of extensive debate. In previous studies of Co-doped samples, small amounts of secondary phases, up to a few percent volume concentration, were found randomly distributed in the matrix material [22–23,30–33]. Keeney *et al.* even found that a 3.95% volume fraction of $CoFe_2O_4$ secondary phase contributed the entire magnetization reported in bulk $Bi_5Ti_3Fe_{0.7}Co_{0.3}O_{15}$ samples [23]. Adding further to the uncertainty, the magnitude of reported net magnetization varies widely among different samples and research groups. For example, the reported saturation magnetization (M_s) and the saturation field (H_s) of Co-doped Aurivillius multiferroic samples are summarized in Table I. Although improvements in the multiferroic coupling of this system are highly desirable, the continued uncertainty regarding the nature and magnitude of the reported FM inhibits future design efforts and greatly limits the potential of Aurivillius-type multiferroics.

The vast majority of magnetization studies of candidate Aurivillius-type multiferroics have been carried out using bulk magnetometry techniques which have the distinct disadvantage that they are sensitive to any net magnetization associated with the sample, whether it be the thin film, contamination within the substrate, or ferromagnetic particulates adhered to the sample. An ideal alternative with which to address this problem is polarized neutron reflectometry (PNR), a powerful tool for probing the magnetism within thin films. Unlike inductive-type magnetometry such as superconducting quantum interference device (SQUID) or vibrating sample magnetometer (VSM), PNR is exclusively sensitive to the structural and magnetic depth profile throughout the thin film heterostructure [42–45]. In this technique, a spin-polarized neutron beam is incident upon the sample and the reflected intensity is measured as a function of the momentum transfer vector along the film normal. Depending on the relative orientation of the neutron spin and any net magnetization within the film, incident neutrons will experience an increase or decrease in the scattering length density (SLD) of the film. Specifically, a neutron with its spin parallel ($\uparrow$) to the magnetization experiences a SLD of (N+M) while a neutron with antiparallel ($\downarrow$) spin experiences a SLD of (N–M), where N is the nuclear SLD and M is the magnetic SLD. Note that the magnetic SLD is directly proportional to the magnetization. Thus, by contrasting the spin-up and spin-down non-spin-flip neutron reflectivity, the nuclear and magnetic depth profiles within the thin film can be elucidated. With the ability to detect weak canted ferromagnetism in a single atomic monolayer in addition to essentially no sensitivity to magnetic ex-

*alexander.grutter@nist.gov

†yllu@ustc.edu.cn

TABLE I. The saturation magnetic field (H_s) and saturation magnetization (M_s) of published Co-doped Aurivillius bulk ceramics and thin films.

Samples	H_S (100 mT) from SQUID	M_S (μ_B/f.u.) from SQUID
$Bi_5Fe_{0.5}Co_{0.5}Ti_3O_{15}$ bulk (Ref. [13])	1	0.003
$Bi_6FeCoTi_3O_{18}$ and $Bi_6LaFeCoTi_3O_{18}$ bulk (Ref. [21])	~5	1.2–1.4
$Bi_5Fe_{0.5}Co_{0.5}Ti_3O_{15}$ bulk with secondary phase (Ref. [22])	~40	0.05
$Bi_6Fe_{1.4}Co_{0.6}Ti_3O_{18}$ polycrystalline film (Ref. [24])	≧40	~1.6
$SrBi_5Fe_{0.5}Co_{0.5}Ti_4O_{18}$ bulk (Ref. [26])	~3	0.81
$Bi_6FeCoTi_3O_{18}$ epitaxial film (Ref. [28])	~4	~0.3
$LaBi_5FeCoTi_3O_{18}$ epitaxial film (Ref. [29])	~7	~0.4
$Bi_{4.25}La_{0.75}Fe_{0.5}Co_{0.5}Ti_3O_{15}$ bulk with secondary phase (Ref. [30])	10	0.258

ternalities, PNR is a unique and powerful tool for detecting the depth-resolved magnetization profile of multilayer structures [46–48]. The combined sensitivity to both structural and magnetic features makes it an ideal way to detect weak magnetism that is often polluted by artifacts. For example, the upper limit of a weak magnetic moment near the $LaAlO_3/SrTiO_3$ interface has been given by a PNR study [49]. PNR study has also been conducted in the multiferroic heterostructures [50,51], ultrathin Fe films during *in situ* growth [52], etc..

To shed light on the origins of magnetism of the Aurivillius thin films, we have studied the magnetic depth profile in high-quality epitaxial thin films of two previously reported RT multiferroic materials, $Bi_6FeCoTi_3O_{18-\delta}$ (BFCTO) and $LaBi_5FeCoTi_3O_{18-\delta}$ (LBFCTO), using PNR. Measurements performed in an applied in-plane field of 700 mT revealed no observable magnetization in the BFCTO film at 300 K, while measurements performed after cooling to 50 K were best fit by a magnetization of $0.049 \pm 0.015\ \mu_B$/Fe-Co pair. Unless otherwise noted, all reported uncertainties represent ± 1 standard deviation. The LBFCTO film, which exhibited a SQUID magnetization of $0.4\ \mu_B$/Fe-Co at RT, yielded similarly suppressed magnetization results through PNR, with a value of $0.016 \pm 0.027\ \mu_B$/Fe-Co. By incorporating PNR and using thin films, which are far less prone to secondary-phase inclusions, our study places tight upper limits on the intrinsic magnetism of the magnetically doped Aurivillius oxides without being influenced by potential magnetic contamination.

Epitaxial thin films of BFCTO and LBFCTO were grown using reflective high-energy electron diffraction (RHEED) assisted pulsed laser deposition (PLD). The targets were prepared with about 10% excess Bi by the citrate combustion method. The $(LaAlO_3)_{0.3}(Sr_2AlTaO_6)_{0.7}$ (LSAT) substrate temperature during growth was 605 °C (thermocouple temperature 680 °C) for BFCTO films and 585 °C (thermocouple temperature 660 °C) for LBFCTO films. The oxygen partial pressure during deposition was 20 Pa. The laser energy was about 100 mJ per pulse and the frequency of the laser pulse was 2 Hz. The stoichiometry of the films was measured by energy dispersive spectrometry (EDS) and x-ray photoemission spectroscopy (XPS), which show the concentrations of the cations being nearly stoichiometric. Our previous x-ray absorption (XAS) experiments show that a small amount of oxygen vacancies exist in both films and the Fe and Co valence is ~3+ and ~2+, respectively [53]. Prior to the deposition of the Aurivillius layers, a thin $LaNiO_3$ buffer layer was deposited on the (001) LSAT substrate. The BFCTO and LBFCTO films were deposited with thicknesses between 50 and 70 nm. The $LaNiO_3$ buffer layer has a thickness of approximately 12 nm. More details of the growth can be found in our previous works [27–29].

The schematic structures of both films are shown in Fig. 1. During the depositions, RHEED was used to monitor the epitaxial growth and no diffraction spots from secondary phases were observed. An x-ray diffraction (XRD) line scan and reciprocal space map measurements demonstrate that both films are coherently strained to the substrate and the layering structure corresponds to the $n = 5$ system as designed. The $(0\,0\,L)$ scans are shown in Figs. 2(a) and 2(b). At room temperature, SQUID vibrating sample magnetometer measurements detected a saturation magnetization of $0.3\ \mu_B$/Fe-Co pair in the BFCTO film with a saturation field of about 4 kOe at RT, as shown in Fig. 2(c). A saturation magnetization of $0.4\ \mu_B$/Fe-Co pair was detected in the LBFCTO film with a saturation field of about 7 kOe at RT. The bare LSAT substrate was measured by SQUID at RT and only a diamagnetic signal was found. The temperature dependence of the magnetization of both films is shown in Fig. 2(d). The ferroelectric properties of these films have been studied in our previous works [28,29]. In this work we focus on the magnetic characterization.

We conducted PNR measurements of the two films at the NIST Center for Neutron Research (NCNR) on the MAGIK and PBR reflectometers at both RT and 50 K with an in-plane applied magnetic field of 700 mT. Incident neutrons were polarized with their spin parallel (↑) or antiparallel (↓) to the field, and the non-spin-flip specular reflectivities ($R^{\uparrow\uparrow}$ and $R^{\downarrow\downarrow}$) were measured as a function of wave vector transfer

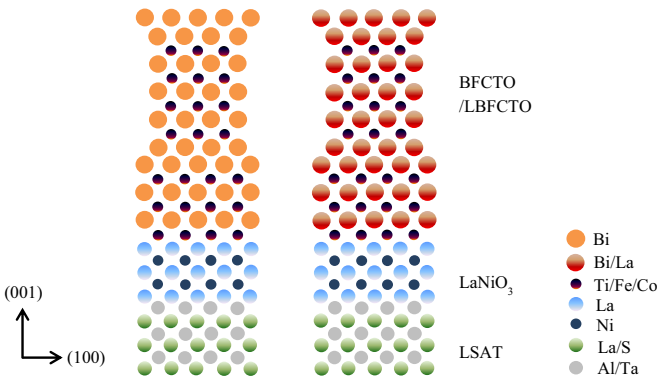

FIG. 1. The schematic structure of the BFCTO and LBFCTO epitaxial films with $LaNiO_3$ buffer layers on (001) LSAT substrates.

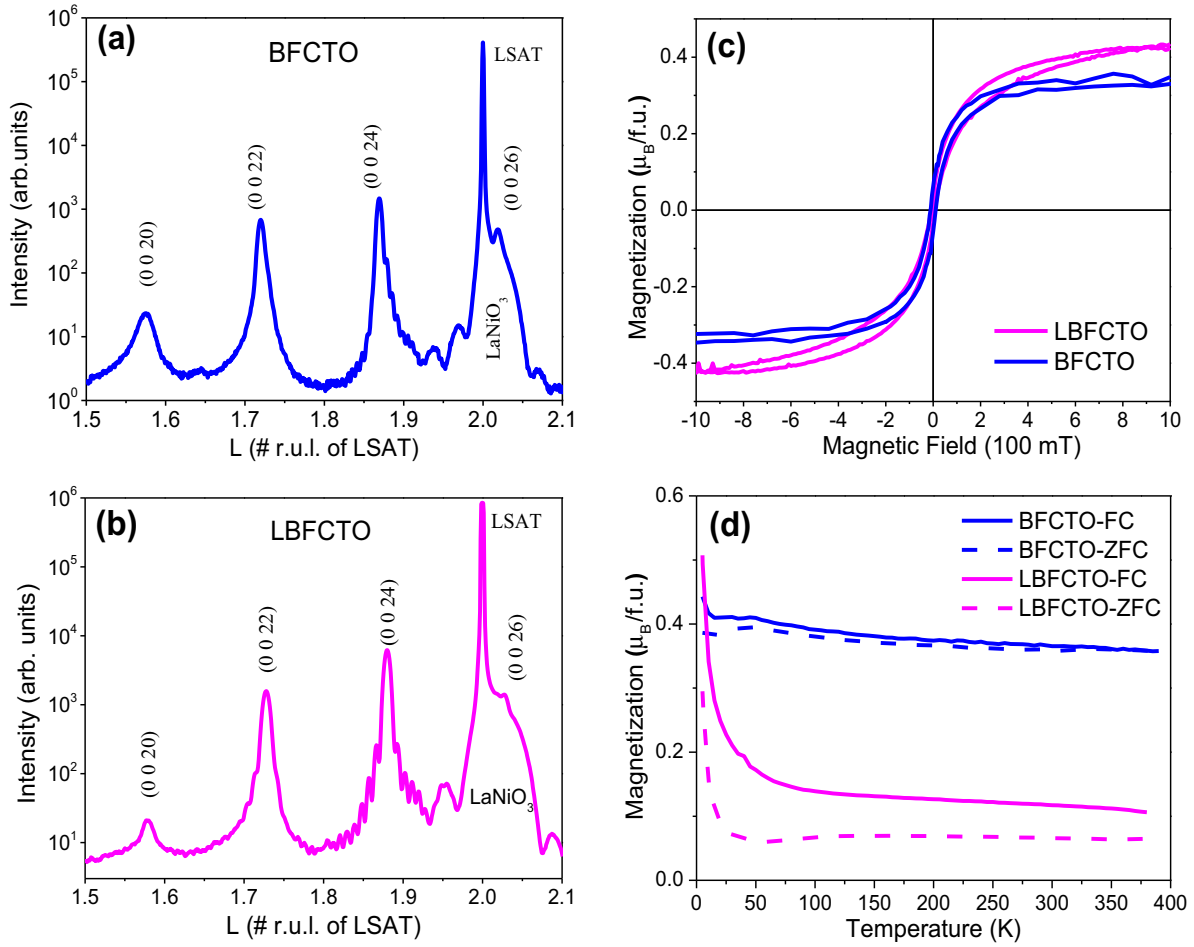

FIG. 2. (a) The XRD (0 0 L) scans of the BFCTO film and (b) the LBFCTO film; (c) the magnetic hysteresis loops of the films measured at room temperature by SQUID; (d) the field cooling (FC) and zero field cooling (ZFC) measurements of the films; the measuring field during warming up was 5000 Oe for the BFCTO film and 100 Oe for the LBFCTO film, respectively.

Q. The SQUID magnetometry results measured at RT show that the applied 700 mT field is large enough to saturate both film magnetizations along the in-plane direction. Thus, no net perpendicular magnetization is expected and the spin-flip reflectivities ($R^{\uparrow\downarrow}$ and $R^{\downarrow\uparrow}$) are not considered here. A useful way of plotting the data which may emphasize particularly weak magnetic features is the spin asymmetry, which is calculated as

$$\mathrm{SA} = \frac{R^{\uparrow\uparrow} - R^{\downarrow\downarrow}}{R^{\uparrow\uparrow} + R^{\downarrow\downarrow}} \propto \frac{(nb+m)^2 - (nb-m)^2}{(nb+m)^2 + (nb-m)^2} \propto \frac{4nbm}{2n^2b^2 + 2m^2},$$

where nb is the Q-dependent Fourier transform of the nuclear SLD and m is the Q-dependent Fourier transform of the magnetic SLD. Thus the SA is sensitive to both the nuclear and magnetic depth profiles, evident by the thickness-dependent oscillations in the data. For small trace magnetization such that $m \ll nb$, the SA reduces to

$$\mathrm{SA} \propto \frac{2m}{nb},$$

so that the spin asymmetry at a given value of Q, SA(Q), is linearly proportional to the magnetization. That is, if the magnetic SLD is much smaller than the nuclear SLD, doubling the magnetization will also double the Q-dependent spin asymmetry, so that magnetization trends may be readily extracted by examining the magnitude of the spin asymmetry features. However, detailed model fitting of the data allows for precise extraction of the depth-dependent nuclear and magnetic SLD and precise uncertainty analysis. Therefore, model fitting of the PNR data was performed using the REFL1D software package and error bars determined by using a Markov chain Monte Carlo method implemented in the BUMPS software package [54]. In the model, the LSAT substrate and the $LaNiO_3$ buffer layers are treated as slabs with uniform nuclear SLD and no magnetic contribution.

The BFCTO film was initially measured at RT in an applied field of 700 mT, at which condition we surprisingly did not observe any measurable difference between $R^{\uparrow\uparrow}$ and $R^{\downarrow\downarrow}$, indicating that the RT magnetization of the film is weaker than the PNR detection limit, as presented in Fig. 3(a). Specifically, fitting the RT data yields a BFCTO magnetization of $0.010 \pm 0.014\,\mu_B$/Fe-Co pair. To demonstrate the sensitivity of our measurement, Fig. 3(b) plots the measured BFCTO spin asymmetry and best fit alongside simulations of alternative models which assume magnetizations consistent with various reports in the literature. As is readily apparent,

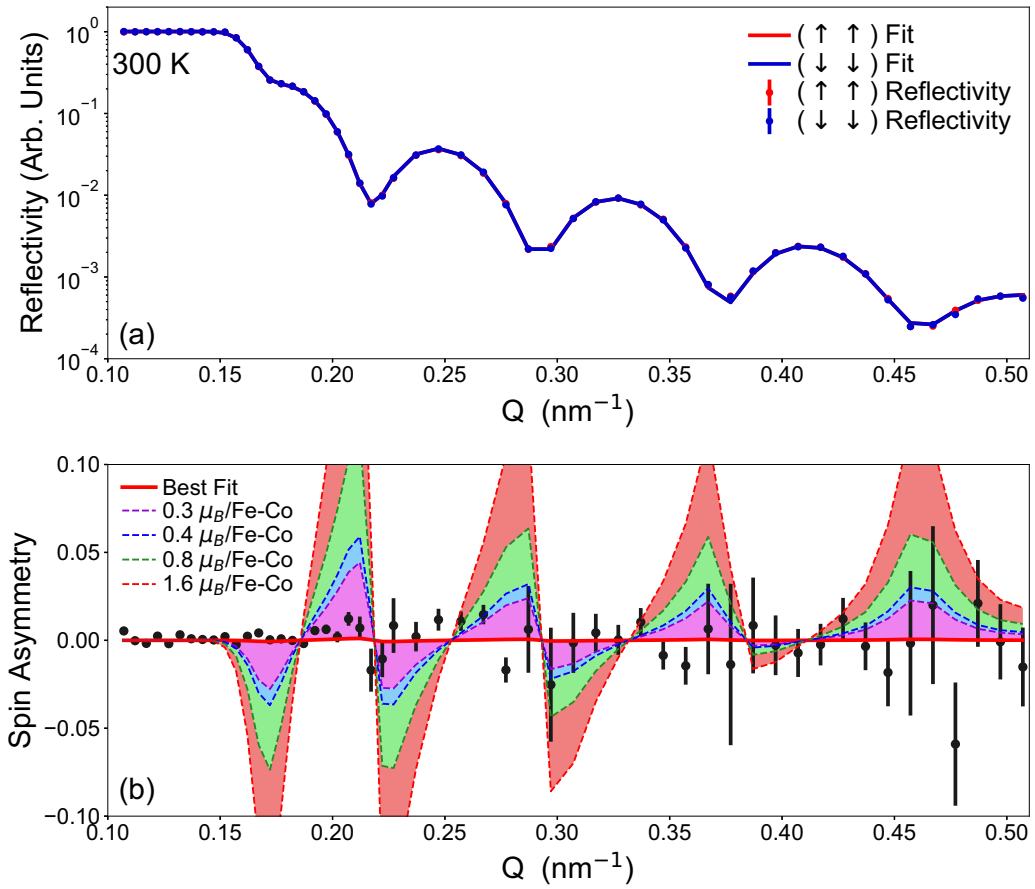

FIG. 3. (a) The spin-dependent $R^{\uparrow\uparrow}$ and $R^{\downarrow\downarrow}$ neutron reflectivities of the BFCTO film at 300 K; (b) the 300 K spin asymmetry (SA) of the BFCTO film. The measurement was done with a 700-mT magnetic field applied along the in-plane direction. Error bars represent ±1 standard deviation.

a RT magnetization of 0.3 μ_B/Fe-Co would be easily detectable and is highly inconsistent with the data. Since no measurable magnetization is apparent at 300 K, we explored a lower temperature measurement where the moment may be enhanced.

When lowering the temperature to 50 K, we observe signatures of an extremely small difference between $R^{\uparrow\uparrow}$ and $R^{\downarrow\downarrow}$ and the emergence of a SA oscillation as a function of Q. Both the raw reflectivity data and the corresponding SA are shown in Figs. 4(a) and 4(b), respectively, alongside the best fit to the data. The extracted structural depth profile plotted in Fig. 4(c) shows excellent agreement with the designed film, with a total thickness of 78 nm including both the BFCTO layer (66 nm) and the $LaNiO_3$ buffer layer (12 nm). Further, we note that both layers appear extremely smooth, with interfacial roughnesses of 1.6 and 1.4 nm at the $LaNiO_3$/BFCTO and BFCTO/air interfaces, respectively. In Fig. 3(b), an extremely weak but statistically significant oscillation of the SA can be observed. Fitting of this dataset yields a net magnetization of 0.049 ± 0.015 μ_B/Fe-Co pair with a 95% confidence interval range from 0.022 μ_B/Fe-Co to 0.078 μ_B/Fe-Co, clearly significantly lower than the SQUID measurement shown in Fig. 2(c), as well as most of the literature examples in Table I. In fact, the only literature reports in Table I which are consistent with this measurement are Refs. [13,22]. However, the bulk SQUID measurement shows a weak magnetic transition near 50 K in Fig. 2(d) of the same film, which agrees with the PNR result. Thus the BFCTO film exhibits an intrinsic weak FM phase below 50 K.

The LBFCTO film with the $LaNiO_3$ buffer layer was measured at RT under the same conditions. Once again, the applied field is sufficient to saturate the magnetization based on the RT hysteresis loop measured by SQUID. The neutron reflectivity data and spin asymmetry for this sample are shown in shown in Figs. 5(a) and 5(b), again exhibiting a thickness oscillation with increasing Q, associated with the total thickness of the LBFCTO and $LaNiO_3$ bilayer. The difference between the $R^{\uparrow\uparrow}$ and $R^{\downarrow\downarrow}$ oscillations is extremely small at RT. The resulting structural and magnetic depth profile is shown in Fig. 5(c), showing excellent agreement with the designed structure. The $LaNiO_3$ thickness is 12.6 nm while the LBFCTO layer thickness is 55 nm. Fitting of this dataset suggests a magnetization of 0.016 ± 0.027 μ_B/Fe-Co with a 95% confidence interval ranging from −0.037 to 0.068 μ_B/Fe-Co. This result is also consistent with Refs. [13,22] but does not allow for any of the larger reported magnetizations.

Thus the PNR measurements place an upper limit on the RT magnetization of 0.08 μ_B/Fe-Co for both BFCTO and LBFCTO thin films. These extracted magnetization values are significantly reduced relative to most values reported in the literature as well as specific SQUID-VSM measurements of these specific films. Our measurements suggest magnetizations

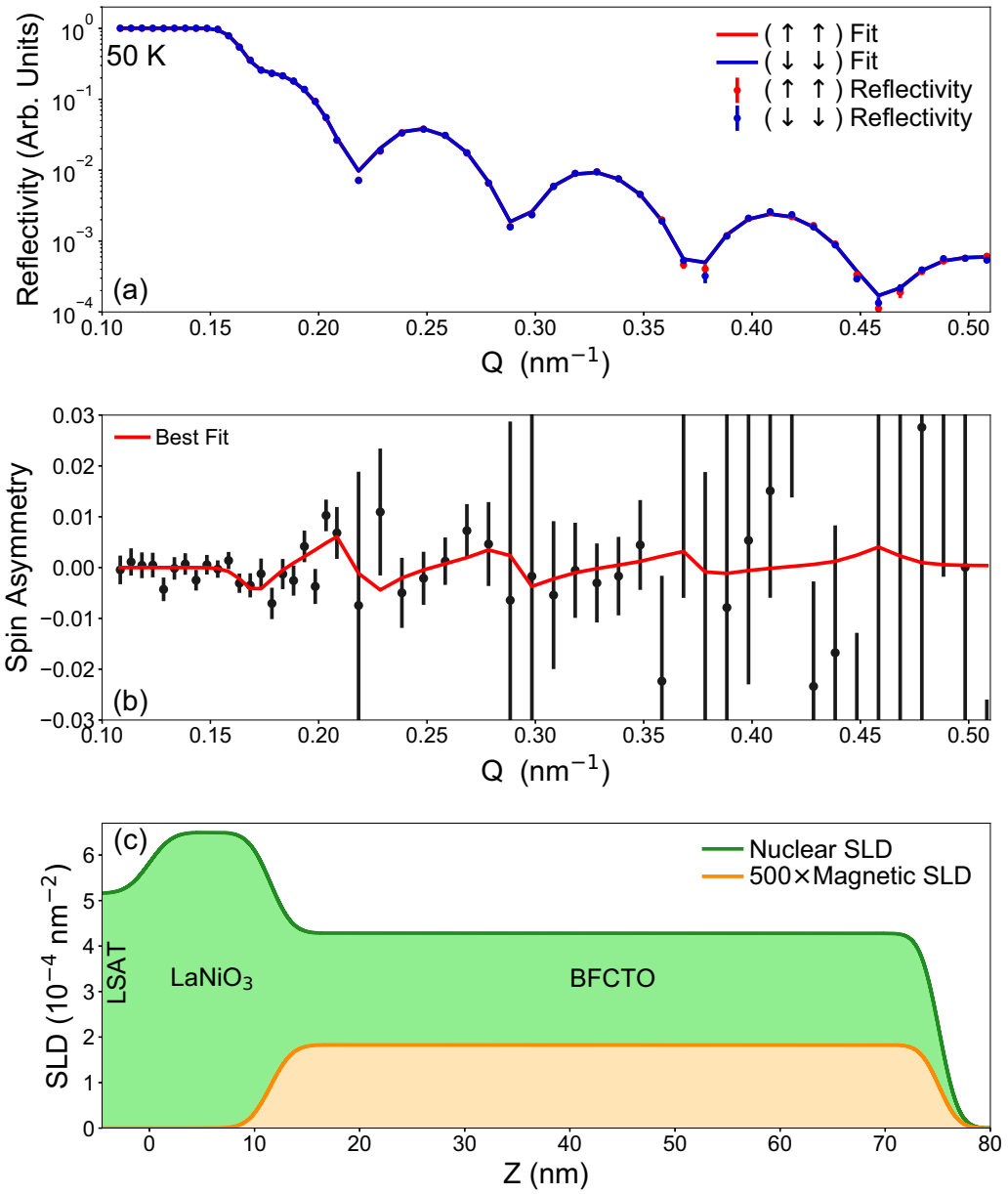

FIG. 4. (a) The 50 K spin-dependent $R^{\uparrow\uparrow}$ and $R^{\downarrow\downarrow}$ neutron reflectivities of the BFCTO film; (b) the 50 K spin asymmetry SA of the BFCTO film. (c) The magnetic and nuclear depth profiles used to obtain the fits shown. The measurement was done with a 700-mT magnetic field applied along the in-plane direction.

which are reduced by more than an order of magnitude relative to many examples in the literature. It indicates that in many cases the reports of enhanced magnetism in these films must instead be attributed to measurement externalities and artifacts associated with bulk magnetometry, namely, substrate contamination, magnetic particulates, or minority phase occlusions within the film itself.

In the case of substrate contamination, the resulting magnetization would almost certainly be sufficiently dilute that it would not be detected by PNR. However, it is also the easiest factor to control for in bulk magnetometry and we therefore suspect this is the least likely source of the contamination. Due to the way in which PNR averages the in-plane SLDs of all the material within the transverse coherence length of a neutron, smaller inclusions would also result in a strong magnetic signal much like a ferromagnetic film [55]. That is, they cannot be distinguished from the film itself and would be detected as a film matrix magnetization which contributes to the spin-dependent splitting. We therefore conclude that small (<200 nm) inclusions of ferromagnetic impurities cannot be responsible for the enhanced magnetization observed in bulk magnetometry. The final possible source of magnetic contamination is larger (>micron scale) particulates. Such contributions would appear in bulk magnetometry but not in the PNR study. Apart from the typical sources of this kind of contamination, pulsed laser deposited samples are particularly susceptible to the deposition of small amounts of ejected particulates from the PLD target, which may include magnetic materials such as Fe oxides. On the other hand, the lack of observable RT FM in the coherent part of the BFCTO and

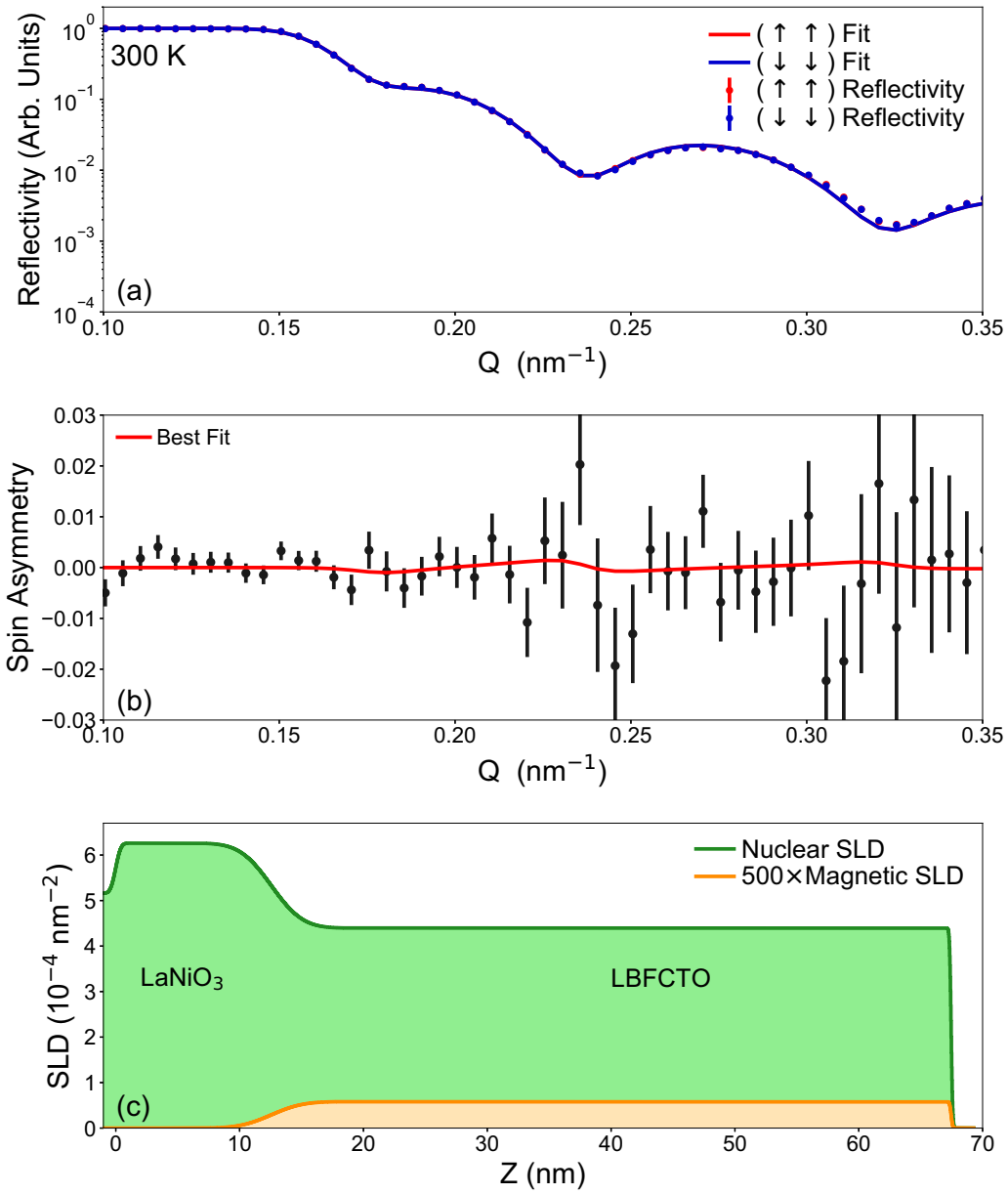

FIG. 5. (a) The 300 K spin-dependent $R^{\uparrow\uparrow}$ and $R^{\downarrow\downarrow}$ neutron reflectivities of the LBFCTO film; (b) the 300 K spin asymmetry SA of the LBFCTO film. (c) The magnetic and nuclear depth profiles used to obtain the fits shown. The measurement was done with a 700-mT magnetic field applied along the in-plane direction.

LBFCTO films might be due to weak or non-FM exchange (between Fe^{3+}-Fe^{3+}, Fe^{3+}-Co^{2+}, Co^{2+}-Co^{2+}), or the low concentration of magnetic ions which weakens long-range magnetic order [56]. The above discussions mainly hold for the Co-doped phase, and phases doped with other magnetic elements may be different.

In conclusion, we have conducted PNR measurements both at RT and low temperature for high-quality epitaxial films of BFCTO and LBFCTO with La doped to the Bi sites. Our study shows that the magnetizations fitted from the depth-dependent PNR results are about one order of magnitude smaller than the magnetization by the macroscopic measurement of SQUID. With sensitivity exclusively limited to the thin film, the PNR method strongly suggests the coherent structure of the BFCTO and LBFCTO films exhibiting at most very weak magnetism at RT and low temperatures. We speculate that the higher reported magnetizations and the wide range of reported values in the literature stem from a tendency to incorporate external sources of magnetic moment into these films during deposition. Our study demonstrates that nonbulk magnetic characterization techniques such as the depth-dependent PNR are critical to revealing the intrinsic magnetic properties of the pure Aurivillius phase in their multiferroic films.

This work used the Extreme Science and Engineering Discovery Environment (XSEDE), which is supported by National Science Foundation Grant No. OCI-1053575. Specifically, it used the Bridges system, which is supported by NSF Award No. ACI-1445606, at the Pittsburgh Supercomputing Center (PSC). The work of the USTC part was supported by the National

Natural Science Foundation of China (Grants No. 11574287 and No. 51627901) and the Fundamental Research Funds for the Central Universities (Grants No. WK2340000065 and No. WK2340000157). X.Z. acknowledges the support of the Youth Innovation Promotion Association CAS (Grant No. 2016389).

[1] N. A. Spaldin and M. Fiebig, Sci. **309**, 391 (2005).
[2] W. Eerenstein, N. D. Mathur, and J. F. Scott, Nature **442**, 759 (2006).
[3] N. A. Hill, J. Phys. Chem. B **104**, 6694 (2000).
[4] C. Ederer and N. A. Spaldin, Phys. Rev. B **71**, 060401(R) (2005).
[5] T. Zhao *et al.*, Nat. Mater. **5**, 823 (2006).
[6] S. Dong, K. Yamauchi, S. Yunoki, R. Yu, S. Liang, A. Moreo, J.-M. Liu, S. Picozzi, and E. Dagotto, Phys. Rev. Lett. **103**, 127201 (2009).
[7] D. H. Wang, W. C. Goh, M. Ning, and C. K. Ong, Appl. Phys. Lett. **88**, 212907 (2006).
[8] H. Béa, M. Bibes, S. Petit, J. Kreisel, and A. Barthélémy, Philos. Mag. Lett. **87**, 165 (2007).
[9] Q.-H. Jiang, C.-W. Nan, and Z.-J. Shen, J. Am. Ceram. Soc. **89**, 2123 (2006).
[10] A. Kumar, I. Rivera, R. S. Katiyar, and J. F. Scott, Appl. Phys. Lett. **92**, 132913 (2008).
[11] Y.-H. Lin, J. Yuan, S. Zhang, Y. Zhang, J. Liu, Y. Wang, and C.-W. Nan, Appl. Phys. Lett. **95**, 033105 (2009).
[12] A. Kumar, R. S. Katiyar, R. N. Premnath, C. Rinaldi, and J. F. Scott, J. Mater. Sci. **44**, 5113 (2009).
[13] X. Mao, W. Wang, X. Chen, and Y. L. Lu, Appl. Phys. Lett. **95**, 082901 (2009).
[14] D. A. Sanchez, A. Kumar, N. Ortega, R. S. Katiyar, and J. F. Scott, Appl. Phys. Lett. **97**, 202910 (2010).
[15] M.-R. Li, U. Adem, S. R. C. McMitchell, Z. Xu, C. I. Thomas, J. E. Warren, D. V. Giap, H. Niu, X. Wan, R. G. Palgrave *et al.*, J. Am. Chem. Soc. **134**, 3737 (2012).
[16] M. Shang, C. Zhang, T. Zhang, L. Yuan, L. Ge, H. Yuan, and S. Feng, Appl. Phys. Lett. **102**, 062903 (2013).
[17] M. J. Pitcher, P. Mandal, M. S. Dyer, J. Alaria, P. Borisov, H. Niu, J. B. Claridge, and M. J. Rosseinsky, Science **347**, 420 (2015).
[18] J. A. Mundy, C. M. Brooks, M. E. Holtz *et al.*, Nature **537**, 523 (2016).
[19] C. M. Fernández-Posada, A. Castro, J.-M. Kiat, F. Porcher, O. Penã, M. Algueró, and H. Amorín, Nat. Commun. **7**, 12772 (2016).
[20] F. J. Yang, P. Su, C. Wei, X. Q. Chen, C. P. Yang, and W. Q. Cao, J. Appl. Phys. **110**, 126102 (2011).
[21] J. Yang, L. H. Yin, Z. Liu, X. B. Zhu, W. H. Song, J. M. Dai, Z. R. Yang, and Y. P. Sun, Appl. Phys. Lett. **101**, 012402 (2012).
[22] M. Palizdar, T. P. Comyn, M. B. Ward *et al.*, J. Appl. Phys. **112**, 073919 (2012).
[23] L. Keeney, S. Kulkarni, N. Deepak *et al.*, J. Appl. Phys. **112**, 052010 (2012).
[24] Z. Liu, J. Yang, X. W. Tang, L. H. Yin, X. B. Zhu, J. M. Dai, and Y. P. Sun, Appl. Phys. Lett. **101**, 122402 (2012).
[25] S. Sun, Y. Huang, G. Wang, J. Wang, Z. Fu, R. Peng, R. J. Knized, and Y. Lu, Nanoscale **6**, 13494 (2014).
[26] J. Wang, Z. Fu, R. Peng, M. Liu, S. Sun, H. Huang, L. Li, R. J. Knize, and Y. L. Lu, Mater. Horiz. **2**, 232 (2015).
[27] Y. Yun, X. Zhai, C. Ma, H. Huang, D. Meng, Z. Cui, J. Wang, Z. Fu, R. Peng, G. J. Brown, and Y. Lu, Appl. Phys. Express **8**, 054001 (2015).
[28] Y. Yun, C. Ma, X. Zhai, H. Huang, D. Meng, J. Wang, Z. Fu, R. Peng, G. J. Brown, and Y. Lu, Appl. Phys. Lett. **107**, 011602 (2015).
[29] Z. Cui, H. Xu, Y. Yun, J. Guo, Y.-D. Chuang, H. Huang, D. Meng, J. Wang, Z. Fu, R. Peng, R. J. Knize, G. J. Brown, X. Zhai, and Y. Lu, J. Appl. Phys. **120**, 084101 (2016).
[30] Z. Li, J. Ma, Z. Gao, G. Viola, V. Koval, A. Mahajan, X. Li, C. Jia, C. Nan, and H. Yan, Dalton Trans. **45**, 14049 (2016).
[31] D. L. Zhang, W. C. Huang, Z. W. Chen, W. B. Zhao, L. Feng, M. Li, Y. W. Yin, S. N. Dong, and X. G. Li, Sci. Rep. **7**, 43540 (2017).
[32] L. Keeney, T. Maity, M. Schmidt, A. Amann, N. Deepak, N. Petkov, S. Roy, M. E. Pemble, and R. W. Whatmore, J. Am. Ceram. Soc. **96**, 2339 (2013).
[33] M. Schmidt, A. Amann, L. Keeney, M.E. Pemble, J. D. Holmes, N. Petkov, and R. W. Whatmore, Sci. Rep. **4**, 5712 (2014).
[34] A. Faraz, T. Maity, M. Schmidt, N. Deepak, S. Roy, M. E. Pemble, R. W. Whatmore, and L. Keeney, J. Am. Ceram. Soc. **100**, 975 (2017).
[35] L. Keeney, C. Downing, M. Schmidt, M. E. Pemble, V. Nicolosi, and R. W. Whatmore, Sci. Rep. **7**, 1737 (2017).
[36] S. Sun, Y. Ling, R. Peng, M. Liu, X. Mao, X. Chen, R. J. Knize, and Y. L. Lu, RSC Adv. **3**, 18567 (2013).
[37] D. Meng, S. Tao, H. Huang, J. Wang, Y. Yun, R. Peng, Z. Fu, L. Zheng, S. Chu, W. Chu, X. Zhai, G. Brown, R. Knize, and Y. Lu, J. Appl. Phys. **121**, 114107 (2017).
[38] J. Yang, W. Tong, Z. Liu, X. B. Zhu, J. M. Dai, W. H. Song, Z. R. Yang, and Y. P. Sun, Phys. Rev. B **86**, 104410 (2012).
[39] R. S. Singh, T. Bhimasankaram, G. S. Kumar, and S. V. Suryanarayana, Solid State Commun. **91**, 567 (1994).
[40] A. Srinivas, S. V. Suryanarayana, G. S. Kumar, and M. Mahesh Kumar, J. Phys.: Condens. Matter **11**, 3335 (1999).
[41] X. W. Dong, K. F. Wang, J. G. Wan, J. S. Zhu, and J.-M. Liu, J. Appl. Phys. **103**, 094101 (2008).
[42] G. P. Felcher, Phys. Rev. B **24**, 1595 (1981).
[43] J. Penfold and R. K. Thomas, J. Phys. Condens. Matter **2**, 1369 (1990).
[44] S. J. Blundell and J. A. C. Bland, Phys. Rev. B **46**, 3391 (1992).
[45] C. A. F. Vaz, J. A. C. Bland, and G. Lauhoff, Rep. Prog. Phys. **71**, 056501 (2008).
[46] A. J. Grutter, B. J. Kirby, M. T. Gray, C. L. Flint, U. S. Alaan, Y. Suzuki, and J. A. Borchers, Phys. Rev. Lett. **115**, 047601 (2015).
[47] S. Roy, M. R. Fitzsimmons, S. Park, M. Dorn, O. Petracic, I. V. Roshchin, Z.-P. Li, X. Batlle, R. Morales, A. Misra *et al.*, Phys. Rev. Lett. **95**, 047201 (2005).
[48] D. A. Gilbert, A. J. Grutter, E. Arenholz, K. Liu, B. J. Kirby, J. A. Borchers, and B. B. Maranville, Nat. Commun. **7**, 12264 (2016).

[49] M. R. Fitzsimmons, N. W. Hengartner, S. Singh, M. Zhernenkov, F. Y. Bruno, J. Santamaria, A. Brinkman, M. Huijben, H. J. A. Molegraaf, J. de la Venta, and I. K. Schuller, Phys. Rev. Lett. **107**, 217201 (2011).

[50] H. Béa, M. Bibes, F. Ott, B. Dupé, X.-H. Zhu, S. Petit, S. Fusil, C. Deranlot, K. Bouzehouane, and A. Barthélémy, Phys. Rev. Lett. **100**, 017204 (2008).

[51] E.-J. Guo, J. R. Petrie, M. A. Roldan, Q. Li, R. D. Desautels, T. Charlton, A. Herklotz, J. Nichols, J, van Lierop, J. W. Freeland, S. V. Kalinin, H. N. Lee, and M. R. Fitzsimmons, Adv. Mater. **29**, 1700790 (2017).

[52] W. Kreuzpaintner, B. Wiedemann, J. Stahn, J.-F. Moulin, S. Mayr, T. Mairoser, A. Schmehl, A. Herrnberger, P. Korelis, M. Haese *et al.*, Phys. Rev. Appl. **7**, 054004 (2017).

[53] Z. Cui, X. Zhai, Y.-D. Chuang, H. Xu, H. Huang, J. Wang, Z. Fu, R. Peng, J. Guo, and Y. Lu, Phys. Rev. B **95**, 205102 (2017).

[54] B. J. Kirby, P. A. Kienzle, B. B. Maranville, N. F. Berk, J. Krycka, F. Heinrich, and C. F. Majkrzak, Curr. Opin. Colloid Interface Sci. **17**, 44 (2012).

[55] C. F. Majkrzak, C. Metting, B. B. Maranville, J. A. Dura, S. Satija, T. Udovic, and N. F. Berk., Phys. Rev. A **89**, 033851 (2014).

[56] A. Birenbaum and C. Ederer, Phys. Rev. B **90**, 214109 (2014).